

Abstract

This study is based on 18 months (20 July 2006–5 February 2008) of continuous measurements of aerosol particle size distributions, air ion size distributions, trace gas concentrations and basic meteorology in a semi-clean savannah environment in Republic of South Africa. New particle formation and growth was observed on 69% of the days and bursts of non-growing ions/sub-10 nm particles on additional 14% of the days. The new particle formation and growth rates were among the highest reported in the literature for continental boundary layer locations; median 10 nm formation rate was $2.2 \text{ cm}^{-3} \text{ s}^{-1}$ and median 10–30 nm growth rate 8.9 nm h^{-1} . The median 2 nm ion formation rate was $0.5 \text{ cm}^{-3} \text{ s}^{-1}$ and the median ion growth rates were 6.2, 8.0 and 8.1 nm h^{-1} for size ranges 1.5–3 nm, 3–7 nm and 7–20 nm, respectively. Three different approaches were used to study the origin of the formation and growth rates: seasonal variation, air mass history analysis and estimated sulphuric acid contribution to the growth. The growth rates had a clear seasonal dependency with minimum during winter and maxima in spring and late summer and the air mass history analysis indicated the highest formation and growth rates to be associated with the area of highest VOC (Volatile Organic Compounds) emissions rather than the highest estimated sulphuric acid concentrations. The relative contribution of estimated sulphuric acid to the growth rate was decreasing with increasing particle size and could explain more than 20% of the observed growth rate only for the 1.5–3 nm size range. The implication is that the sulphuric acid alone is not enough to explain the growth, but the highest growth rates seem to originate in VOC emissions following from biological activity. The frequency of new particle formation, however, increased nearly monotonously with the estimated sulphuric acid reaching 100% at H_2SO_4 concentration of $4 \times 10^7 \text{ cm}^{-3}$, which suggests the formation and growth to be independent of each other.

New particle formation events in semi-clean South African savannah

V. Vakkari et al.

Title Page

Abstract

Introduction

Conclusions

References

Tables

Figures

⏪

⏩

◀

▶

Back

Close

Full Screen / Esc

Printer-friendly Version

Interactive Discussion



1 Introduction

The aerosol particles affect the radiation budget in two ways: directly by scattering the solar radiation and indirectly via acting as cloud condensation nuclei and therefore modulating the properties of the clouds. Besides that aerosol particles affect significantly also human health and visibility in urban areas (Pope and Dockery, 2006; Hand and Malm, 2007; Anderson, 2009). Actually the largest current uncertainties in the anthropogenic changes in the Earth radiation budget arise from aerosols – the uncertainty in the total aerosol effect on earth radiative forcing is larger than the combined effect of the long-lived greenhouse gases CO₂ and methane (Forster et al., 2007).

To reduce the uncertainty of the aerosol effects on global radiation budget measurements of the atmospheric aerosols have to be conducted globally, because the aerosol population in the atmosphere is largely inhomogeneous due to the relatively short atmospheric lifetime of the aerosol particles. Therefore regional conditions, as well as seasonal changes in the regional conditions, have a large effect on processes which affect the regional aerosol properties.

The concentrations of climatically important aerosol particles are due to their different sources and sinks. The sources of the aerosol particles in the size range where they can effectively contribute to the direct or indirect radiative effect include primary emissions from natural processes, anthropogenic primary emissions and new particle formation from gaseous compounds in the atmosphere, which has been observed in a variety of environments around the globe (Kulmala et al., 2004). The importance of new particle formation to the global aerosol budget has also been confirmed by global models (Spracklen et al., 2008).

Although the need is evident, there is only a limited amount of aerosol observations from Africa (Swap et al., 2003) and other less developed areas (Laakso et al., 2006). On the other hand, the number of long-term continuous measurements of aerosol particle properties in Europe and North America, observations are increasing (e.g., Manninen et al., 2010). For instance the only reported observations of new particle formation

New particle formation events in semi-clean South African savannah

V. Vakkari et al.

Title Page

Abstract

Introduction

Conclusions

References

Tables

Figures



Back

Close

Full Screen / Esc

Printer-friendly Version

Interactive Discussion

New particle formation events in semi-clean South African savannah

V. Vakkari et al.

Title Page

Abstract

Introduction

Conclusions

References

Tables

Figures

⏪

⏩

◀

▶

Back

Close

Full Screen / Esc

Printer-friendly Version

Interactive Discussion



and growth from continental Africa so far are by Laakso et al. (2008), who gave an overview of the first complete year of the measurements in Botsalano game reserve in North-West Province in Republic of South Africa. Laakso et al. (2008) reported new particle formation to take place on almost every sunny day with formation and growth rates among the highest observed in continental environments. Therefore the paper concluded that new particle formation in savannah environment is likely to have a regional effect on cloud condensation nucleus budget and on the properties of the clouds.

In this study, supporting the EUCAARI project South African component (Kulmala et al., 2009), we give a more detailed analysis on the new particle formation observed on background savannah (Laakso et al., 2008). The measurements utilized in this study are for the period 20 July 2006–5 February 2008 with the main focus being on aerosol particle and air ion formation and growth rates. The seasonal variation of the formation and growth rates is studied and, in order to understand the processes behind the observations, the measurements are combined with air mass history analysis, ion recombination calculations and estimates of sulphuric acid concentrations using a recently developed proxy (Petäjä et al., 2009).

2 Measurements

2.1 Measurement location

The measurements for this study were conducted in Botsalano game reserve (Laakso et al., 2008), latitude 25.54° S, longitude 25.75° E, 1400 m a.s.l., from 20 July 2006 until 5 February 2008.

Botsalano game reserve is located in the North-West Territory of the Republic of South Africa, Fig. 1, 10 km from the border of Botswana and 50 km from the nearest towns, Mafikeng, population 260 000, in the south and Zeerust, population 140 000, in the east. Gaborone, population 200 000, capital of Botswana, lies 100 km north of measurement site and Rustenburg, population 400 000, 150 km east of the site.

New particle formation events in semi-clean South African savannahV. Vakkari et al.

[Title Page](#)[Abstract](#)[Introduction](#)[Conclusions](#)[References](#)[Tables](#)[Figures](#)[Back](#)[Close](#)[Full Screen / Esc](#)[Printer-friendly Version](#)[Interactive Discussion](#)

The region east of Botsalano is quite sparsely populated next to the game reserve, but has heavy industry in the Rustenburg area. Rustenburg is considered as one of the large regional pollution sources in the North-West Province (Piketh et al., 2005; Laakso et al., 2008) due to its large platinum group metal mines and refineries. Other major sources in the east impacting the measurement site are the megacity of Johannesburg approximately 220 km east with more than 10 million inhabitants, and especially the industrialized Highveld southeast of Johannesburg with high emissions from coal-based power plants and petrochemical industry.

The region west and south of Botsalano, on the Botswana side and the Karoo region in South Africa, has little industrial or other anthropogenic activities and forms the clean sector. In addition to industrial sources, the site is affected by emissions from regular wild fires during the dry season (June–October). The major fires are in the north; however, fires may take place in any direction from the site.

2.2 Instrumentation

The mobile measurement trailer and the instrumentation in the trailer are described in detail by Petäjä et al. (2010). In this study we utilize aerosol particle size distributions from the differential mobility particle sizer (DMPS) (Hoppel, 1978; Jokinen and Mäkelä, 1997), size range 10–840 nm, air ion size distributions from the air ion spectrometer (AIS) (Mirme et al., 2007), size range 0.8–42 nm, sulphur dioxide concentration from the Thermo 42S analyser (Thermo Environmental Instruments Inc., 1992) and the basic meteorological quantities including solar radiation from the photosynthetically active radiation (PAR) sensor (LiCor LI-190SB).

3 Methods

3.1 New particle formation classification

New particle formations events were determined in the DMPS measurements along the guidelines set in Dal Maso et al. (2005). The aerosol particle size distribution data from the DMPS measurements was divided in new particle formation or “event days”, “non-event days”, when no new particles were formed and “undefined days”, when it was not possible to determine with complete certainty whether there was new particle formation or not.

To classify a day as a new particle formation day, new particles were required to appear in the size range smaller than 25 nm and the new mode was required to grow in mean diameter. These days were further divided into three sub-categories IA, IB and II, depending on how smooth the size distribution was. For the classes IA and IB it was possible to calculate formation and growth rates from the measurements, whereas for class II determination of one or the other was not possible due for instance to gaps or fluctuations in the size distribution.

New particle formation was determined from the ion spectra obtained from AIS measurements according to the classification presented by Yli-Juuti et al. (2009). The five main classes, see above, were the same for ions and aerosol particle spectra from the DMPS, but in addition four more classes were defined to describe some characteristics typical for the ion spectrum but not seen in DMPS. These extra classes belong to the undefined category in the DMPS aerosol particle classification. The detailed new particle formation classification criteria are presented in Table 1.

Ion bursts caused by rain in sizes 1–25 nm (Hirsikko et al., 2007) were encountered frequently during the wet season and the so called Mixed-type ion bursts throughout the period, but the classes Apple and Hump are included in the study mainly for consistency with earlier studies by Vana et al. (2008) and Yli-Juuti et al. (2009). Days when there were gaps in the data so that they could not reliably be classified in above classes were classified as bad data and left out from the analysis.

New particle formation events in semi-clean South African savannah

V. Vakkari et al.

Title Page

Abstract

Introduction

Conclusions

References

Tables

Figures

⏪

⏩

◀

▶

Back

Close

Full Screen / Esc

Printer-friendly Version

Interactive Discussion



3.2 Aerosol particle formation and growth rates

The 10 nm aerosol particle formation rate – the 10 nm set by the DMPS detection limit – and the aerosol particle growth rate were determined from DMPS measurements similarly as in Dal Maso et al. (2005), who expressed

$$J_{10} = \frac{dN_{10-30}}{dt} + F_{\text{coag}} + F_{\text{growth}}. \quad (1)$$

The first term, $\frac{dN_{10-30}}{dt}$, was obtained from a linear fit to the 10–30 nm particle concentration during the time at the beginning of the new particle formation when the concentration increase is nearly linear. The coagulation loss term, F_{coag} , was calculated according to the formulae given by Dal Maso et al. (2005) and the last term, F_{growth} , representing the losses from particles growing out of the size range, was taken to equal zero, as the 10–30 nm size range is wide enough so that the particles do not grow past the upper limit of the size range during the period when formation rate is determined.

For the growth rate calculation Dal Maso et al. (2005) used a log-normal size distribution fit to the measured aerosol particle size spectrum to follow the time evolution of the distribution. Now a one to three modal log-normal fit was calculated using a method described in detail by Vartiainen et al. (2007).

The actual growth rate is obtained by tracing the maximum of the log-normal fit to the nucleation mode as it grows from 10 to 30 nm and making a linear fit to the obtained data points. The upper limit for the growth rate calculation was increased from the 25 nm used by Dal Maso et al. (2005) to 30 nm because of the high growth rates observed (Laakso et al., 2008). Only the modal peaks above the 10 nm detection limit of the DMPS were used for calculating the growth rate – fitting a mode when most of the mode is outside the measurement range can lead to ambiguous results.

New particle formation events in semi-clean South African savannah

V. Vakkari et al.

Title Page

Abstract

Introduction

Conclusions

References

Tables

Figures

⏪

⏩

◀

▶

Back

Close

Full Screen / Esc

Printer-friendly Version

Interactive Discussion



3.3 Formation and growth rates of charged particles and ions

The charged particle and ion formation and growth rates were determined according to Kulmala et al. (2007) and Hirsikko et al. (2005).

The 2 nm ion formation rate J_2^\pm obtained from the AIS measurements was calculated according to Kulmala et al. (2007) as

$$J_2^\pm = \frac{dN^\pm}{dt} + \text{CoagS}_{2-3} \cdot N^\pm + \frac{\text{GR}^\pm}{3\text{nm} - 2\text{nm}} \cdot N^\pm + \alpha \cdot N^\pm \cdot N_{<3\text{nm}}^\mp - \beta \cdot N \cdot N_{<3\text{nm}}^\pm, \quad (2)$$

where \pm refers to the polarity of the ions, N^\pm to 2–3 nm ion concentration of respective polarity, N to the concentration of 2–3 nm neutral particles, CoagS_{2-3} to the coagulation sink for 2–3 nm particles, GR^\pm to the growth rate of respective polarity 1.5–3 nm ions, α to the ion-ion recombination coefficient and β to the ion-aerosol recombination coefficient.

The first term, $\frac{dN^\pm}{dt}$, was calculated similarly as for the 10 nm formation rate, i.e. by a linear fit to the concentration of 2–3 nm ions. GR^\pm was calculated for the size interval 1.5–3 nm as described below. For the calculation of J_2^\pm N was assumed to be a hundred times the sum of the total 2–3 nm ion concentration N^\pm as recent observations from boreal forest suggest (Manninen et al., 2009a). The values for coefficients α and β were $1.6 \times 10^{-6} \text{ cm}^3 \text{ s}^{-1}$ and $0.01 \times 10^{-6} \text{ cm}^3 \text{ s}^{-1}$ (Tamm et al., 2005). The total 2 nm ion formation rate $J_2(\text{ions})$ is the sum of positive and negative ion formation rates.

The ion-ion recombination yield of neutral 2–3 nm particles was calculated similarly as in Manninen et al. (2009b). The recombination rate was calculated for the complete measurement period. For the new particle formation events ion-ion recombination rate is given as median value during the linear growth of the 2–3 nm ion concentration, i.e. the period when the first term in Eq. (2) was defined. The upper limit of ion induced nucleation was estimated as a sum of recombination rate and the total ion formation rate $J_2(\text{ions})$.

New particle formation events in semi-clean South African savannah

V. Vakkari et al.

Title Page

Abstract

Introduction

Conclusions

References

Tables

Figures

⏪

⏩

◀

▶

Back

Close

Full Screen / Esc

Printer-friendly Version

Interactive Discussion



New particle formation events in semi-clean South African savannah

V. Vakkari et al.

Title Page

Abstract

Introduction

Conclusions

References

Tables

Figures

◀

▶

◀

▶

Back

Close

Full Screen / Esc

Printer-friendly Version

Interactive Discussion



The AIS ion spectra were analysed for the growth rates using the method described by Hirsikko et al. (2005) by following the position of the maximum concentration (in time) for each size channel of the AIS in a size interval. For the ion spectrum three size regions were selected for calculating the growth rate: 1.5–3 nm, 3–7 nm and 7–20 nm.

5 These are commonly used to account for the change of growth rate during the growth of the particles and were used also by Hirsikko et al. (2005).

To compare the 10–30 nm particle growth rate with the corresponding growth rate obtained from AIS measurements, we determined the 10–30 nm ion growth rate using the log-normal fitting method described for DMPS measurements in Sect. 3.2. For
10 the comparison also the formation rate of 10 nm ions was determined with the same method as applied to the DMPS spectrum.

3.4 Sulphuric acid proxy

Sulphuric acid concentration was estimated with a proxy calculated according to the Eq. (4) by Petäjä et al. (2009) as

$$15 \quad \text{H}_2\text{SO}_4 \text{ proxy} = k_3 \frac{[\text{SO}_2] \cdot \text{Glob}}{\text{CS}}, \quad (3)$$

where SO_2 is the measured sulphur dioxide concentration, Glob is the measured global radiation, CS is the condensation sink calculated from the aerosol particle size distribution measured with the DMPS (see Dal Maso et al., 2005) and the empirical scaling factor (Petäjä et al., 2009)

$$20 \quad k_3 = 8.4 \times 10^{-8} \cdot \text{Glob}^{-0.68}. \quad (4)$$

This sulphuric acid proxy has been developed based on measurements in boreal forest and thus the absolute values are not necessary valid for Southern African conditions. Despite this significant uncertainty, it provides valuable information on the spatial variability and annual cycles of sulphuric acid.

3.5 Air mass history

The air mass history was investigated using back-trajectories. The back-trajectories were calculated using the HYbrid Single-Particle Lagrangian Integrated Trajectory (HYSPLIT) version 4.8 model developed by the National Oceanic and Atmospheric Administration (NOAA) Air Resources Laboratory (ARL) (Draxler and Hess, 2004). The model was run with the GDAS meteorological archive produced by the US National Weather Service's National Centre for Environmental Prediction (NCEP) and archived by ARL (Air Resources Laboratory, 2009). The HYSPLIT model was run for 96-h back-trajectories at every hour throughout the complete measurement period.

The accuracy of trajectories greatly depends on the quality of the underlying meteorological data in use (Stohl, 1998). The errors accompanying single trajectories are currently estimated as 15 to 30% of the trajectory distance travelled (Stohl, 1998; Rid-dle et al., 2006). Studying regional patterns and using a large dataset this accuracy is sufficient.

For the air mass history study the Southern Africa was divided to a $0.5^{\circ} \times 0.5^{\circ}$ grid. Each back-trajectory was assigned the parameters observed at the measurement site when the trajectory arrived. The grid cells were then allocated an average value of the observed quantities assigned to the trajectories passing through the cell. A minimum of five trajectories per cell was required for the statistical reliability.

4 Results

4.1 New particle formation and growth rates

New particle formation and growth was observed on 69% of the days during the measurement period 20 July 2006–5 February 2008. In addition to this, on 14% of the days, non-growing ion bursts were observed. This reanalysis of the data shows lower values than the 90% new particle formation frequency reported by Laakso et al. (2008), but the new particle formation frequency in Botsalano is still the highest reported from

ACPD

10, 30777–30821, 2010

New particle formation events in semi-clean South African savannah

V. Vakkari et al.

Title Page

Abstract

Introduction

Conclusions

References

Tables

Figures

⏪

⏩

◀

▶

Back

Close

Full Screen / Esc

Printer-friendly Version

Interactive Discussion



continental boundary layer so far. On only 6% of the days there certainly was no new particle formation, which leaves 11% of the days as undefined. The new particle formation frequency did not have seasonal variation but remained rather constant throughout the measurement period, Fig. 2.

The growth rates determined from the DMPS measurements varied from 2.1 to 30 nm h⁻¹ with the mean of 9.7 nm h⁻¹ and median 8.9 nm h⁻¹. The annual behaviour of the growth rates is presented in Fig. 3. For January and February the values are averaged over 2007 and 2008 and for July to December over 2006 and 2007. The growth rate clearly peaks in spring and late summer, from September to November and February, and has a minimum in winter, from May to August. This is in accordance with earlier observations from Northern Hemisphere (e.g., Kulmala et al., 2004; Dal Maso et al., 2005) where the seasonal variation of particle growth rates is explained by changes in biogenic VOC-emissions (e.g., Mäkelä et al., 1997; Dal Maso et al., 2005). In case of Southern Africa, the similar annual biogenic emission cycle can be explained by precipitation pattern and respective changes in vegetation (Otter et al., 2002, 2003; Güenther et al., 1996).

The formation rate of 10 nm particles, J_{10} , from the DMPS measurements varied from 0.1 to 28 cm⁻³ s⁻¹ with mean of 3.8 cm⁻³ s⁻¹ and median 2.2 cm⁻³ s⁻¹. Also the annual behaviour of the J_{10} shows peaks in the spring and in the late summer and a minimum during the winter, which is in line with previous observations in Northern Hemisphere (e.g., Dal Maso et al., 2005). This is likely to be caused by the seasonal difference in the growth rate as with higher growth rate a bigger fraction of the nucleated 1–2 nm particles get to grow to 10 nm instead of being scavenged by larger particles.

The ion growth rates were determined from the AIS measurements for three size ranges, 1.5–3 nm, 3–7 nm and 7–20 nm. The mean, minimum and maximum values are given in Table 2. Monthly averages of these growth rates are presented in Fig. 4 left panel. The values for each month are averaged over both polarities. The new particle formation was not always as clear in the smallest size range of 1.5–3 nm as in larger sizes and thus that size range has fewer observations than the larger size

New particle formation events in semi-clean South African savannah

V. Vakkari et al.

Title Page

Abstract

Introduction

Conclusions

References

Tables

Figures

⏪

⏩

◀

▶

Back

Close

Full Screen / Esc

Printer-friendly Version

Interactive Discussion

ranges. The number of events analysed for GR is presented for each month in the left panel of the Fig. 4.

The ion growth rates show the same shape of annual behaviour as DMPS in all size ranges, that is, a maximum during the spring and in the summer and a minimum in the winter. Between February and May 2007 the AIS data coverage was limited due to instrument maintenance and customs problems. During the whole measurement period the growth rate of 3–7 nm ions was highest with the most pronounced annual cycle. The seasonal variation of the growth rate of 1.5–3 nm ions is the smallest in the three size ranges.

The seasonal behaviour of the 2 nm ion formation rate, $J_2(\text{ions})$, is presented in the right panel of Fig. 4. The $J_2(\text{ions})$ does not have much of a seasonal variation. The $J_2(\text{ions})$ has been calculated as a sum of positive and negative J_2 for the days when it was possible to calculate growth rate of 1.5–3 nm ions. The fifth term in Eq. (2), which carries the assumption of the neutral cluster concentration being hundred times the measured total ion cluster concentration, is on average 25% (maximum 90%) of the sum of the terms 1–4 in Eq. (2). The values of $J_2(\text{ions})$ range from 0.07 to 1.6 $\text{cm}^{-3} \text{s}^{-1}$ with mean of 0.5 $\text{cm}^{-3} \text{s}^{-1}$. The formation rate of neutral 2 nm clusters from the ion-ion recombination was on average 0.3 $\text{cm}^{-3} \text{s}^{-1}$ during new particle formation periods and 0.03 $\text{cm}^{-3} \text{s}^{-1}$ during the whole period. The upper limit of ion induced nucleation calculated as sum of $J_2(\text{ions})$ and ion-ion recombination is on average 0.8 $\text{cm}^{-3} \text{s}^{-1}$.

Figure 5 presents the growth and formation rates for both polarities separately. The annual behaviour of the polarities does not have significant differences except that the positive ion J_2 seems to be slightly elevated during the spring.

To study the seasonal variation in the condensation sink the median CS was calculated daily for period 09:30–10:30 LT, which is the hour following the median observed new particle formation onset. The CS is clearly elevated during the dry season from May to October with highest values before the beginning of the rainy season in September, Fig. 6. The all time average of the CS was $4.3 \times 10^{-3} \text{s}^{-1}$ during the measurement period.

New particle formation events in semi-clean South African savannah

V. Vakkari et al.

[Title Page](#)[Abstract](#)[Introduction](#)[Conclusions](#)[References](#)[Tables](#)[Figures](#)[⏪](#)[⏩](#)[◀](#)[▶](#)[Back](#)[Close](#)[Full Screen / Esc](#)[Printer-friendly Version](#)[Interactive Discussion](#)

methods as for the DMPS. The observed linear dependency indicates that the measurements with DMPS and AIS are consistent although the operation principles are not identical.

4.2 Sulphuric acid

5 New particle formation frequency was calculated as a function of estimated sulphuric acid concentration by dividing the concentration into logarithmically evenly spaced bins and calculating the frequency of new particle formation and growth – i.e. days classified as IA, IB or II according to Table 1 – in each bin. Also the frequency of non-event days was calculated in each bin. The estimated sulphuric acid concentration was calculated
10 as the median during the first hour after the observed onset of the formation for event days. For all other days the concentration was calculated as the median during 09:30–10:30 LT, because 09:30 is the median of the observed formation onset times.

The effect of sulphuric acid on new particle formation frequency is illustrated in Fig. 9, which clearly indicates how increasing sulphuric acid concentration increases the frequency of new particle formation and growth and correspondingly decreases the frequency of non-event days. At concentrations higher than 2×10^7 molecules cm^{-3} we do not observe any more non-event days and above 4×10^7 molecules cm^{-3} there are only
15 clear new particle formation and growth days.

The sulphuric acid contribution to the growth rate of aerosol particles was estimated using the following simple relations: for particles smaller than 3 nm, a concentration of 6×10^6 molecules of H_2SO_4 corresponds to 1 nm h^{-1} growth rate, for particles between 3 and 7 nm 1×10^7 molecules of H_2SO_4 corresponds to 1 nm h^{-1} growth rate and for particles larger than 7 nm 1.37×10^7 molecules of H_2SO_4 corresponds to 1 nm h^{-1}
20 growth rate (Kulmala, 1988; Kulmala et al., 2001).

New particle formation events in semi-clean South African savannah

V. Vakkari et al.

Title Page

Abstract

Introduction

Conclusions

References

Tables

Figures

⏪

⏩

◀

▶

Back

Close

Full Screen / Esc

Printer-friendly Version

Interactive Discussion

New particle formation events in semi-clean South African savannah

V. Vakkari et al.

[Title Page](#)[Abstract](#)[Introduction](#)[Conclusions](#)[References](#)[Tables](#)[Figures](#)[⏪](#)[⏩](#)[◀](#)[▶](#)[Back](#)[Close](#)[Full Screen / Esc](#)[Printer-friendly Version](#)[Interactive Discussion](#)

The estimated sulphuric acid calculated according to Petäjä et al. (2009) has a clear seasonal cycle in Botsalano with maximum during the dry season from May to July, Fig. 10. This cycle is nearly the opposite of the cycle of the 10–30 nm aerosol particle growth rates, which is also seen in the fraction of observed 10–30 nm growth rate explained by the estimated sulphuric acid, Fig. 11. However, the fraction of 10–30 nm growth rate explained by the estimated sulphuric acid is at maximum only around 16–17%, so clearly sulphuric acid alone cannot explain the observed aerosol particle growth. For this comparison the estimated sulphuric acid values are medians for the period when the growth rates are determined.

In the smaller size range growth rates from the AIS measurements the fraction of growth rate explained by the estimated sulphuric acid is increasing with decreasing size, but the seasonal dependency seems to vanish, Fig. 11. On average, the estimated sulphuric acid concentration can explain 33% of the 1.5–3 nm growth rate, 16% of the 3–7 nm growth rate, 12% of the 7–20 nm growth rate and 12% of the 10–30 nm growth rate.

4.3 The effect of air mass history on growth and formation rates

Figure 12 gives an overview of the meteorological patterns in Botsalano. The anticyclonic flow around the Highveld area (Garstang et al., 1996) is clearly the dominant flow pattern. The semi-permanent continental anticyclone leads to air re-circulating over the sub-continent from a week up to 20 days (Tyson et al., 1996). During the dry season this re-circulation together with long-lasting temperature inversion preventing vertical mixing of the air causes the atmosphere to be often layered with alternating layers of clean air and air polluted from industrial sources or from biomass burning (Hobbs, 2003).

The high SO₂ emissions from the industry in the Highveld, see discussion in Sect. 2.1, show clearly on the SO₂ source areas based on the air mass history, Fig. 13. The emissions from the Highveld are so large that they screen the emissions before the Highveld and even generate artificial sources due south of Botsalano, Fig. 13 left

New particle formation events in semi-clean South African savannah

V. Vakkari et al.

Title Page

Abstract

Introduction

Conclusions

References

Tables

Figures



Back

Close

Full Screen / Esc

Printer-friendly Version

Interactive Discussion

side. Therefore all back-trajectories passing over the highest sources in the Highveld – the blue polygon in Fig. 13 right-hand map – were cut so that the tail of the back trajectory before it passed over Highveld was left out from the analysis. This removes the artificial sources in the left-hand map in Fig. 13 and results in the right-hand map.

5 This map compares well with the SO₂ emission inventory, Fig. 1. Sources of SO₂ on the south western coast over 1000 km away from Botsalano (in Western Cape) are not visible, but otherwise the SO₂ source areas follow the shape of the emission inventory. The same cut was applied to air mass history studies of aerosol particles and other variables as well.

10 The highest aerosol particle formation and growth rates determined from the DMPS measurements show up in the north-easterly directions from the Botsalano game reserve, Fig. 14. This is the region where the VOC emission inventory by Otter (2004) presents the highest monoterpenes emissions. The semi-arid Karoo region southwest of Botsalano produces slightly lower growth rates and clearly lower formation rates.

15 The Highveld and the Rustenburg–Johannesburg area east of Johannesburg do not stand out as high growth or formation rate sources even though the highest SO₂ concentrations originate in these areas, Fig. 13.

The 2 nm ion formation rates show a same kind of pattern as the 10 nm aerosol particle formation rate, Fig. 15. The highest ion formation rates originate in the North-Eastern Limpopo valley whereas the South-Western Karoo direction yields clearly lower formation rates. The areas with most anthropogenic activities show formation rates slightly below average.

20 The ion growth rates are also generally smaller when air masses are coming from the South-Western Karoo direction and higher for the north-eastern direction, Fig. 16. The 1.5–3 nm negative ion growth rate, however, has a maximum at the Rustenburg–Johannesburg area and the 3–7 nm growth rates of both polarities show slightly elevated values for the Rustenburg–Johannesburg area. The difference in 1.5–3 nm growth rates may be related to ion chemistry favouring condensation of sulphuric acid on negative ions.

The 7–20 nm ion growth rates follow the same pattern as the 10–30 nm aerosol particle growth rates with highest growth rates originating in the north-eastern direction and the lowest from the south-western direction.

The condensation sink source areas have same kind of general pattern as the aerosol particle growth rate. The South-Western Karoo region produces a very low condensation sink whereas the highest values of CS originate in the northern and eastern directions. The highest CS values come, however, from the Highveld region, Fig. 17, not the North-Eastern Limpopo valley where the highest growth rates originate.

The source area distribution of the estimated sulphuric acid is presented in Fig. 18. The highest concentrations originate quite naturally in the areas of highest SO₂ emissions, i.e. the Highveld region east of Johannesburg. In the south western direction the concentrations are the lowest.

The contribution of sulphuric acid to the growth rate is largest for all size ranges for air masses originating in the Highveld region and smallest for the south-western direction, Fig. 19. The decrease in the relative significance of H₂SO₄ with increasing size is clearly seen. The estimated sulphuric acid can explain over 25% of the 10–30 nm growth rate only for air masses coming from the Johannesburg–Highveld region whereas for the smallest size range, 1.5–3 nm, it can explain a major fraction of the observed growth also for air masses coming from the north-eastern direction and occasionally also from the south-western direction. However, one should keep in mind that the sulphuric acid concentration is only indicative as it is estimated based on a proxy developed for a different environment.

5 Conclusions

We have presented here the first detailed analysis on new particle formation in semi-clean savannah environment based on one and half years of continuous measurements of air ions, aerosol particle size distribution, trace gases and basic meteorological variables. New particle formation and growth was observed on 69% of the days. In

New particle formation events in semi-clean South African savannah

V. Vakkari et al.

Title Page

Abstract

Introduction

Conclusions

References

Tables

Figures



Back

Close

Full Screen / Esc

Printer-friendly Version

Interactive Discussion



originated in the same area as the highest SO₂ and estimated sulphuric acid concentrations whereas the highest 3–7 nm and 7–20 nm ion and 10–30 nm aerosol particle growth rates originated in the same region where the VOC emission inventory by Otter (2004) presents the highest monoterpene emissions.

The three different approaches used to study the origin of the observed high growth rates – seasonal variation, sulphuric acid estimates and source areas – all indicate that sulphuric acid alone is not enough to explain the growth. The seasonal variation and the source areas suggest the growth to originate in VOC emissions following from biological activity. On the other hand, the occurrence of new particle formation and growth was strongly dependent on sulphuric acid and the contribution of sulphuric acid to the growth immediately after nucleation was significant, which implies that the formation and growth processes are to a large degree independent of each other.

Acknowledgements. The authors acknowledge the financial support by the Academy of Finland under the projects Air pollution in Southern Africa (APSA) (project number 117505) and Atmospheric monitoring capacity building in Southern Africa (project number 132640) and by the European Commission 6th Framework program project EUCAARI, contract no 036833-2 (EUCAARI). The authors thank Head of Botsalano game reserve, M. Khukhela and the game reserve employees for their kind and invaluable help during our measurements. In addition, the authors are grateful to M. Jokinen and E. Sjöberg for their help to organizing the project.

References

- Air Resources Laboratory: Gridded Meteorological Data Archives, available at: <http://www.arl.noaa.gov/archives.php>, accessed 17.3.2009.
- Anderson, H. R.: Air pollution and mortality: a history, *Atmos. Environ.*, 43, 142–152, 2009.
- Cantrell, C. A.: Technical Note: Review of methods for linear least-squares fitting of data and application to atmospheric chemistry problems, *Atmos. Chem. Phys.*, 8, 5477–5487, doi:10.5194/acp-8-5477-2008, 2008.
- Dal Maso, M., Kulmala, M., Riipinen, I., Wagner, R., Hussein, T., Aalto, P. P., and Lehtinen, K. E. J.: Formation and growth of fresh atmospheric aerosols: eight years of aerosol

New particle formation events in semi-clean South African savannah

V. Vakkari et al.

Title Page

Abstract

Introduction

Conclusions

References

Tables

Figures



Back

Close

Full Screen / Esc

Printer-friendly Version

Interactive Discussion



New particle formation events in semi-clean South African savannah

V. Vakkari et al.

Title Page

Abstract

Introduction

Conclusions

References

Tables

Figures

⏪

⏩

◀

▶

Back

Close

Full Screen / Esc

Printer-friendly Version

Interactive Discussion

size distribution data from SMEAR II, Hyytiälä, Finland, *Boreal Environ. Res.*, 10, 323–336, 2005.

Draxler, R. R. and Hess, G. D.: Description of the HYSPLIT_4 Modelling System, NOAA Technical Memorandum ERL ARL–224, Air Resources Laboratory, Silver Spring, Maryland, 2004.

5 Fleming, G. and van der Merwe, M.: Spatial disaggregation of greenhouse gas emissions inventory data for Africa south of the equator, available at: <http://gis.esri.com/library/userconf/proc00/professional/papers/PAP896/p896.htm>, last access: 7 September 2010, 2002.

10 Forster, P., Ramaswamy, V., Artaxo, P., Bernsten, T., Betts, R., Fahey, D. W., Haywood, J., Lean, J., Lowe, D. C., Myhre, G., Nganga, J., Prinn, R., Raga, G., Schulz, M., and Van Dorland, R.: Changes in atmospheric constituents and in radiative forcing, in: *Climate Change 2007: The Physical Science Basis. Contribution of Working Group I to the Fourth Assessment Report of the Intergovernmental Panel on Climate Change*, edited by: Solomon, S., Qin, D., Manning, M., Chen, Z., Marquis, M., Averyt, K. B., Tignor, M., and Miller, H. L., Cambridge University Press, Cambridge and New York, NY, 136, 2007.

15 Garstang, M., Tyson, M., Swap, R., Edwards, M., Kållberg, P., and Lindesay, J. A.: Horizontal and vertical transport of air over Southern Africa, *J. Geophys. Res.*, 101, 23721–23736, 1996.

20 Güenther, A., Otter, L., Zimmermann, P., Greenberg, J., Scholes, R., and Scholes, M.: Biogenic hydrocarbon emissions from Southern African savannas, *J. Geophys. Res.*, 101, 25859–25865, 1996.

Hand, J. L. and Malm, W. C.: Review of aerosol mass scattering efficiencies from ground-based measurements since 1990, *J. Geophys. Res.*, 112, D16203, doi:10.1029/2007JD008484, 2007.

25 Hirsikko, A., Laakso, L., Hörrak, U., Aalto, P. P., Kerminen, V.-M., and Kulmala, M.: Annual and size dependent variation of growth rates and ion concentration in boreal forest, *Boreal Environ. Res.*, 10, 357–369, 2005.

Hirsikko, A., Bergman, T., Laakso, L., Dal Maso, M., Riipinen, I., Hörrak, U., and Kulmala, M.: Identification and classification of the formation of intermediate ions measured in boreal forest, *Atmos. Chem. Phys.*, 7, 201–210, doi:10.5194/acp-7-201-2007, 2007.

30 Hobbs, P. V.: Clean air slots amid dense atmospheric pollution in Southern Africa, *J. Geophys. Res.*, 108, 8490, doi:10.1029/2002JD002156, 2003.

Hoppel, W. A.: Determination of the aerosol size distribution from the mobility distribution of the charged fraction of aerosols, *J. Aerosol Sci.*, 9, 41–54, 1978.

New particle formation events in semi-clean South African savannah

V. Vakkari et al.

[Title Page](#)[Abstract](#)[Introduction](#)[Conclusions](#)[References](#)[Tables](#)[Figures](#)[⏪](#)[⏩](#)[◀](#)[▶](#)[Back](#)[Close](#)[Full Screen / Esc](#)[Printer-friendly Version](#)[Interactive Discussion](#)

- lida, K., Stolzenburg, M., McMurry, P., Dunn, M. J., Smith, J. N., Eisele, F., and Keady, P.: Contribution of ion-induced nucleation to new particle formation: methodology and its application to atmospheric observations in Boulder, Colorado, *J. Geophys. Res.*, 111, D23201, doi:10.1029/2006JD007167, 2006.
- 5 Jokinen, V. and Mäkelä, J. M.: Closed loop arrangement with critical orifice for DMA sheath/excess flow system, *J. Aerosol Sci.*, 28, 643–648, 1997
- Kulmala, M.: Nucleation as an aerosol physical problem, Ph.D. thesis, University of Helsinki, Helsinki, Finland, 1988.
- Kulmala, M., Dal Maso, M., Mäkelä, J. M., Pirjola, L., Väkevää, M., Aalto, P., Miiikkulainen, P., Hämeri, K., and O'Dowd, C.: On the formation, growth and composition of nucleation mode particles, *Tellus B*, 53, 479–490, 2001.
- 10 Kulmala, M., Vehkamäki, H., Petäjä, T., Dal Maso, M., Lauri, A., Kerminen, V.-M., Birmili, W., and McMurry, P. H.: Formation and growth rates of ultrafine atmospheric particles: a review of observations, *J. Aerosol Sci.*, 35, 143–176, 2004.
- 15 Kulmala, M., Riipinen, I., Sipilä, M., Manninen, H. E., Petäjä, T., Junninen, H., Dal Maso, M., Mordas, G., Mirme, A., Vana, M., Hirsikko, A., Laakso, L., Harrison, M. M., Hanson, I., Leung, C., Lehtinen, K. E. J., and Kerminen, V.-M.: Toward direct measurement of atmospheric nucleation, *Science*, 318, 89–92, 2007.
- Kulmala, M., Asmi, A., Lappalainen, H. K., Carslaw, K. S., Pöschl, U., Baltensperger, U., Hov, Ø., Brenquier, J.-L., Pandis, S. N., Facchini, M. C., Hansson, H.-C., Wiedensohler, A., and O'Dowd, C. D.: Introduction: European Integrated Project on Aerosol Cloud Climate and Air Quality interactions (EUCAARI) – integrating aerosol research from nano to global scales, *Atmos. Chem. Phys.*, 9, 2825–2841, doi:10.5194/acp-9-2825-2009, 2009.
- 20 Laakso, L., Koponen, I. K., Mönkkönen, P., Kulmala, M., Kerminen, V.-M., Wehner, B., Wiedensohler, A., Wu, Z., and Hu, M.: Aerosol particles in the developing world; a comparison between New Delhi in India and Beijing in China, *Water Air Soil Poll.*, 173, 5–20, 2006.
- 25 Laakso, L., Gagné, S., Petäjä, T., Hirsikko, A., Aalto, P. P., Kulmala, M., and Kerminen, V.-M.: Detecting charging state of ultra-fine particles: instrumental development and ambient measurements, *Atmos. Chem. Phys.*, 7, 1333–1345, doi:10.5194/acp-7-1333-2007, 2007.
- 30 Laakso, L., Laakso, H., Aalto, P. P., Keronen, P., Petäjä, T., Nieminen, T., Pohja, T., Siivola, E., Kulmala, M., Kgabi, N., Molefe, M., Mabaso, D., Phalatse, D., Pienaar, K., and Kerminen, V.-M.: Basic characteristics of atmospheric particles, trace gases and meteorology in a relatively clean Southern African Savannah environment, *Atmos. Chem. Phys.*, 8, 4823–4839,

New particle formation events in semi-clean South African savannah

V. Vakkari et al.

Title Page

Abstract

Introduction

Conclusions

References

Tables

Figures

⏪

⏩

◀

▶

Back

Close

Full Screen / Esc

Printer-friendly Version

Interactive Discussion

doi:10.5194/acp-8-4823-2008, 2008.

Mäkelä, J. M., Aalto, P., Jokinen, V., Pohja, T., Nissinen, A., Palmroth, S., Markkanen, T., Seitsonen, K., Lihavainen, H., and Kulmala, M.: Observations of ultrafine aerosol particle formation and growth in boreal forest, *Geophys. Res. Lett.*, 24, 1219–1222, 1997.

5 Manninen, H. E., Petäjä, T., Asmi, E., Riipinen, I., Nieminen, T., Mikkilä, J., Hörrak, U., Mirme, A., Mirme, S., Laakso, L., Kerminen, V.-M., and Kulmala, M.: Long-term field measurements of charged and neutral clusters using Neutral cluster and Air Ion Spectrometer (NAIS), *Boreal Environ. Res.*, 14, 591–605, 2009a.

10 Manninen, H. E., Nieminen, T., Riipinen, I., Yli-Juuti, T., Gagné, S., Asmi, E., Aalto, P. P., Petäjä, T., Kerminen, V.-M., and Kulmala, M.: Charged and total particle formation and growth rates during EUCAARI 2007 campaign in Hyytiälä, *Atmos. Chem. Phys.*, 9, 4077–4089, doi:10.5194/acp-9-4077-2009, 2009b.

15 Manninen, H. E., Nieminen, T., Asmi, E., Gagné, S., Häkkinen, S., Lehtipalo, K., Aalto, P., Vana, M., Mirme, A., Mirme, S., Hörrak, U., Plass-Dülmer, C., Stange, G., Kiss, G., Hoffer, A., Törö, N., Moerman, M., Henzing, B., de Leeuw, G., Brinkenberg, M., Kouvarakis, G. N., Bougiatioti, A., Mihalopoulos, N., O'Dowd, C., Ceburnis, D., Arneth, A., Svenningsson, B., Swietlicki, E., Tarozzi, L., Decesari, S., Facchini, M. C., Birmili, W., Sonntag, A., Wiedensohler, A., Boulon, J., Sellegri, K., Laj, P., Gysel, M., Bukowiecki, N., Weingartner, E., Wehrle, G., Laaksonen, A., Hamed, A., Joutsensaari, J., Petäjä, T., Kerminen, V.-M., and Kulmala, M.: EUCAARI ion spectrometer measurements at 12 European sites – analysis of new particle formation events, *Atmos. Chem. Phys.*, 10, 7907–7927, doi:10.5194/acp-10-7907-2010, 2010.

20 Mirme, A., Tamm, E., Mordas, G., Vana, M., Uin, J., Mirme, S., Bernotas, T., Laakso, L., Hirsikko, A., and Kulmala, M.: A wide-range multi-channel Air Ion Spectrometer, *Boreal Environ. Res.*, 12, 247–264, 2007.

25 Otter, L.: SAFARI 2000 Estimated BVOC Emissions for Southern African Land Cover Types, Data Set, available at: <http://daac.ornl.gov/>, last access: 19 March 2009, from Oak Ridge National Laboratory Distributed Active Archive Centre, Oak Ridge, Tennessee, USA, 2004.

30 Otter, L. B., Güenther A., and Greenberg, J.: Seasonal and spatial variations in biogenic hydrocarbon emissions from Southern African savannas and woodlands, *Atmos. Environ.*, 36, 4265–4275, 2002.

Otter, L., Güenther, A., Wiedinmyer, C., Fleming, G., Harley, P., and Greenberg, J.: Spatial and temporal variations in biogenic volatile organic compound emissions for Africa south of equator, *J. Geophys. Res.*, 108, 8505, doi:10.1029/2002JD002609, 2003.

- Petäjä, T., Mauldin, III, R. L., Kosciuch, E., McGrath, J., Nieminen, T., Paasonen, P., Boy, M., Adamov, A., Kotiaho, T., and Kulmala, M.: Sulfuric acid and OH concentrations in a boreal forest site, *Atmos. Chem. Phys.*, 9, 7435–7448, doi:10.5194/acp-9-7435-2009, 2009.
- Petäjä, T., Vakkari, V., Pohja, T., Nieminen, T., Laakso, H., Aalto, P. P., Keronen, P., Siivola, E., Kerminen, V.-M., Kulmala, M., and Laakso, L.: Transportable air quality and atmospheric monitoring trailer for developing countries: design, instruments and verification, submitted to *Boreal Environ. Res.*, 2010.
- Piketh, S., van Nierop, M., Rautenbach, C., Walton, N., Ross, K., Holmes, S., and Richards, T.: Rustenburg local municipality air quality management plan, palace consulting engineers ltd., Randburg, Republic of South Africa, 2005.
- Pope, C. A. and Dockery, D. W.: Health effects of fine particulate air pollution: lines that connect, *J. Air Waste Manage.*, 56, 709–742, 2006.
- Riddle, E. E., Voss, P. B., Stohl, A., Holcomb, D., Maczka, D., Washburn, K., and Talbot, R. W.: Trajectory model validation using newly developed altitude-controlled balloons during the International Consortium for Atmospheric Research on Transport and Transformations 2004 campaign, *J. Geophys. Res.*, 111, D23S57, doi:10.1029/2006JD007456, 2006.
- Spracklen, D. V., Carslaw, K. S., Kulmala, M., Kerminen, V.-M., Sihto, S.-L., Riipinen, I., Merikanto, J., Mann, G. W., Chipperfield, M. P., Wiedensohler, A., Birmili, W., and Lihavainen, H.: Contribution of particle formation to global cloud condensation nuclei concentrations, *Geophys. Res. Lett.*, 35, L06808, doi:10.1029/2007GL033038, 2008.
- Stohl, A.: Computation, accuracy and application of trajectories – a review and bibliography, *Atmos. Environ.*, 32, 947–966, 1998.
- Swap, R. J., Annegarn, H. J., Suttles, J. T., King, M. D., Platnick, S., Privette, J. L., and Scholes, R. J.: Africa burning: a thematic analysis of the Southern African Regional Science Initiative (SAFARI 2000), *J. Geophys. Res.*, 108, 8465, doi:10.1029/2003JD003747, 2003
- Tammet, H. and Kulmala, M.: Simulation tool for atmospheric aerosol nucleation bursts, *J. Aerosol Sci.*, 36, 173–196, 2005.
- Thermo Environmental Instruments, Inc.: Instruction Manual for Model 43S High Sensitive Pulsed Fluorescence SO₂ Analyzer, Thermo Environ. Instruments, Inc., Franklin, MA, USA, 1992.
- Tyson, P. D., Garstang, M., and Swap, R.: Large-scale recirculation of air over Southern Africa, *J. Appl. Meteorol.*, 35, 2218–2236, 1996.

New particle formation events in semi-clean South African savannah

V. Vakkari et al.

[Title Page](#)[Abstract](#)[Introduction](#)[Conclusions](#)[References](#)[Tables](#)[Figures](#)[⏪](#)[⏩](#)[◀](#)[▶](#)[Back](#)[Close](#)[Full Screen / Esc](#)[Printer-friendly Version](#)[Interactive Discussion](#)

New particle formation events in semi-clean South African savannah

V. Vakkari et al.

[Title Page](#)[Abstract](#)[Introduction](#)[Conclusions](#)[References](#)[Tables](#)[Figures](#)[⏪](#)[⏩](#)[◀](#)[▶](#)[Back](#)[Close](#)[Full Screen / Esc](#)[Printer-friendly Version](#)[Interactive Discussion](#)

Vana, M., Ehn, M., Petäjä, T., Vuollekoski, H., Aalto, P. P., de Leeuw, G., Ceburnis, D., O'Dowd, C. D., and Kulmala, M.: Characteristic features of air ions at Mace Head on the west coast of Ireland, *Atmos. Res.*, 90, 278–286, 2008.

5 Vartiainen, E., Kulmala, M., Ehn, M., Hirsikko, A., Junninen, H., Petäjä, T., Sogacheva, L., Kuokka, S., Hillamo, R., Skorokhod, A., Belikov, I., Elansky, N., and Kerminen, V.-M.: Ion and particle number concentrations and size distributions along the Trans-Siberian railroad, *Boreal Environ. Res.*, 12, 375–396, 2007.

10 Yli-Juuti, T., Riipinen, I., Aalto, P. P., Nieminen, T., Maenhaut, W., Janssens, I. A., Claeys, M., Salma, I., Ocskay, R., Hoffer, A., Imre, K., and Kulmala, M.: Characteristics of new particle formation events and cluster ions at K-pusztá, Hungary, *Boreal Environ. Res.*, 14, 683–698, 2009.

York, D., Evensen, N. M., López Martínez, M., and De Basabe Delgado, J.: Unified equations for the slope, intercept, and standard errors of the best straight line, *Am. J. Phys.*, 7, 367–375, 2004.

New particle formation events in semi-clean South African savannah

V. Vakkari et al.

Title Page

Abstract

Introduction

Conclusions

References

Tables

Figures

⏪

⏩

◀

▶

Back

Close

Full Screen / Esc

Printer-friendly Version

Interactive Discussion



Table 1. New particle formation criteria. The ion burst criteria, the four last classes, are reproduced after Yli-Juuti et al. (2009).

IA DMPS and AIS	New mode with growing mean diameter appears in particle size range smaller than 25 nm. No or little fluctuation in mode particle number and mean diameter. Low background concentration, suitable for modelling studies.
IB DMPS and AIS	New mode with growing mean diameter appears in particle size range smaller than 25 nm. Possible to calculate growth rate.
II DMPS and AIS	New mode with growing mean diameter appears in particle size range smaller than 25 nm. Disturbances in the growth of the new mode or in the data make it impossible to determine growth rate.
Non-event DMPS and AIS	No new particles appear below 25 nm and no growing Aitken-size mode.
Undefined DMPS and AIS	Uncertain days when it cannot be determined with full certainty if there was new particle formation or not. New particles appear below 25 nm but do not grow.
Apple AIS only	There is a new mode below 25 nm but the mean diameter of the mode does not grow. There is a clear gap between the new mode and other modes.
Hump AIS only	There is a nucleation burst starting from the cluster mode but the growth does not continue to larger sizes than 10 nm.
Rain AIS only	Rain-induced ion bursts in nucleation mode size range.
Mixed-type AIS only	There are new particles in the size range smaller than 25 nm. The day does not have features of class I, II, apple or hump, or it has features of many of these classes.

New particle formation events in semi-clean South African savannah

V. Vakkari et al.

Table 2. The mean, minimum and maximum for the growth and formation rates of aerosol particles and ions. The ion growth rates are averaged over both polarities. Total ions indicates the sum of J_2 (ions) and ion-ion recombination rate and is an approximation of the upper limit of the ion induced nucleation.

	Mean	Median	25 percentile	75 percentile	Min	Max
GR_{10-30} [nm h ⁻¹]	9.7	8.9	6.3	12	2.1	30
$GR_{1.5-3}^{\pm}$ [nm h ⁻¹]	7.5	6.2	4.3	9.3	1.4	31
GR_{3-7}^{\pm} [nm h ⁻¹]	9.9	8.0	5.4	12	1.3	60
GR_{7-20}^{\pm} [nm h ⁻¹]	8.9	8.1	5.3	11	2.0	29
J_{10} [cm ⁻³ s ⁻¹]	3.8	2.2	1.0	4.4	0.1	28
J_2^- [cm ⁻³ s ⁻¹]	0.2	0.2	0.1	0.3	0.02	0.9
J_2^+ [cm ⁻³ s ⁻¹]	0.2	0.2	0.1	0.3	0.02	1.1
J_2 (ions) [cm ⁻³ s ⁻¹]	0.5	0.5	0.3	0.6	0.07	1.6
Ion-ion recombination rate [cm ⁻³ s ⁻¹]	0.3	0.2	0.1	0.4	0.01	1.7
Total ions [cm ⁻³ s ⁻¹]	0.8	0.7	0.5	1.0	0.1	2.4

[Title Page](#)
[Abstract](#)
[Introduction](#)
[Conclusions](#)
[References](#)
[Tables](#)
[Figures](#)
[⏪](#)
[⏩](#)
[◀](#)
[▶](#)
[Back](#)
[Close](#)
[Full Screen / Esc](#)
[Printer-friendly Version](#)
[Interactive Discussion](#)


New particle formation events in semi-clean South African savannah

V. Vakkari et al.

Title Page

Abstract

Introduction

Conclusions

References

Tables

Figures

◀

▶

◀

▶

Back

Close

Full Screen / Esc

Printer-friendly Version

Interactive Discussion

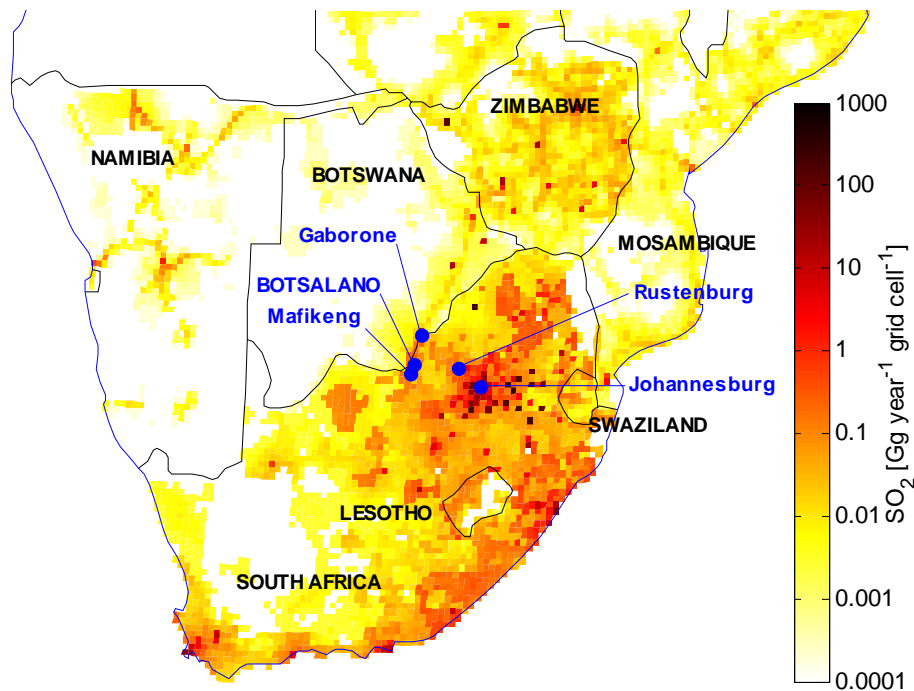


Fig. 1. Location of Botsalano game reserve and SAFARI 2000 SO_2 emission inventory (Fleming and van der Merwe, 2002). The resolution of the emission inventory is 20 km.

New particle formation events in semi-clean South African savannah

V. Vakkari et al.

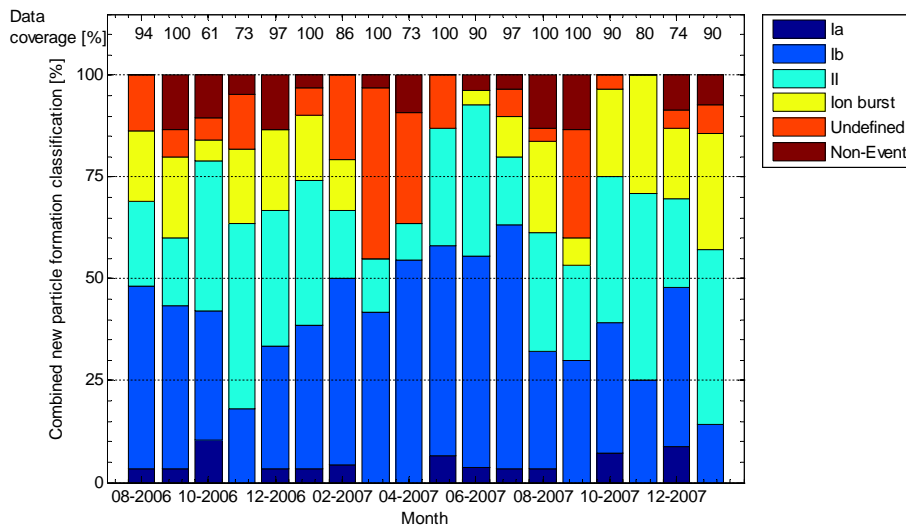


Fig. 2. New particle formation frequency combined from both DMPS and AIS measurements. Classes I and II show clear new particle formation and growth. Ion bursts include all periods when non-growing ions were observed in the 2–25 nm size range.

[Title Page](#)
[Abstract](#)
[Introduction](#)
[Conclusions](#)
[References](#)
[Tables](#)
[Figures](#)
[⏪](#)
[⏩](#)
[◀](#)
[▶](#)
[Back](#)
[Close](#)
[Full Screen / Esc](#)
[Printer-friendly Version](#)
[Interactive Discussion](#)

New particle formation events in semi-clean South African savannah

V. Vakkari et al.

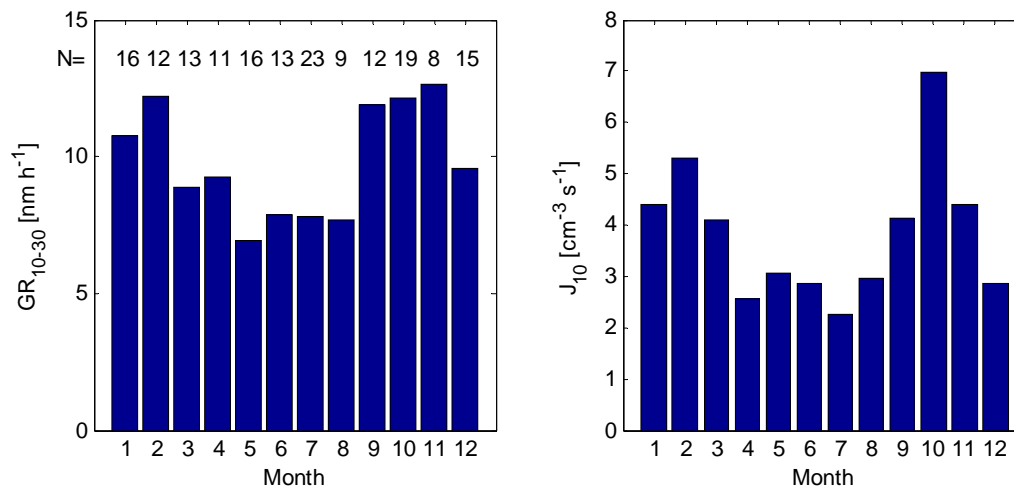


Fig. 3. Annual behaviour of aerosol particle formation and growth rates averaged over 18 months. Number of events analysed for each month is indicated in the left hand side panel.

[Title Page](#)[Abstract](#)[Introduction](#)[Conclusions](#)[References](#)[Tables](#)[Figures](#)[⏪](#)[⏩](#)[◀](#)[▶](#)[Back](#)[Close](#)[Full Screen / Esc](#)[Printer-friendly Version](#)[Interactive Discussion](#)

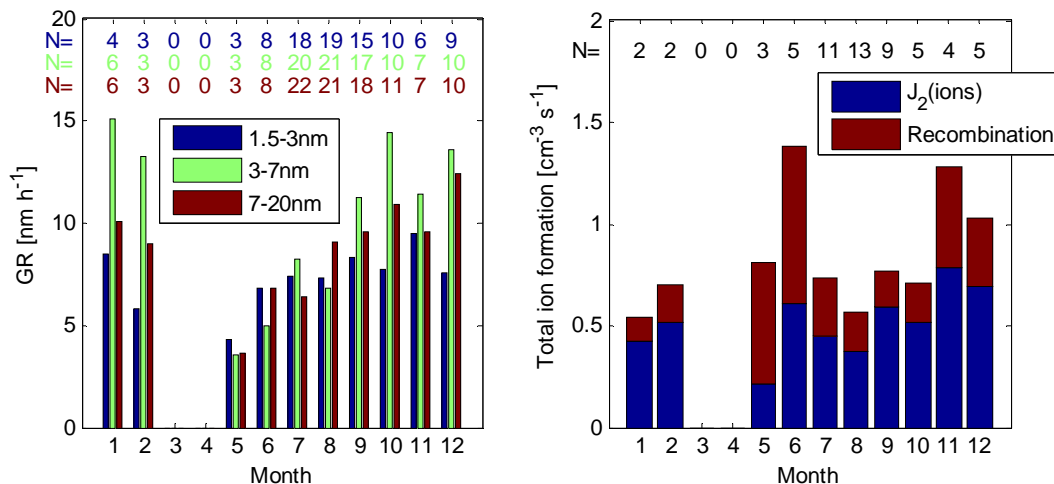


Fig. 4. The left panel of the figure presents the monthly averages of the ion growth rates from the AIS measurements for three size ranges. The growth rates are averaged over both polarities. The seasonal variation is strongest in the 3–7 nm size range. The right panel presents the ion formation rate $J_2(\text{ions})$ and the ion-ion recombination rate, which give an estimate of the upper limit of the ion formation (e.g., Manninen et al., 2009b). The formation rate does not have a seasonal dependence. The number of events analysed for each month and size range are also shown.

New particle formation events in semi-clean South African savannah

V. Vakkari et al.

Title Page

Abstract

Introduction

Conclusions

References

Tables

Figures

◀

▶

◀

▶

Back

Close

Full Screen / Esc

Printer-friendly Version

Interactive Discussion

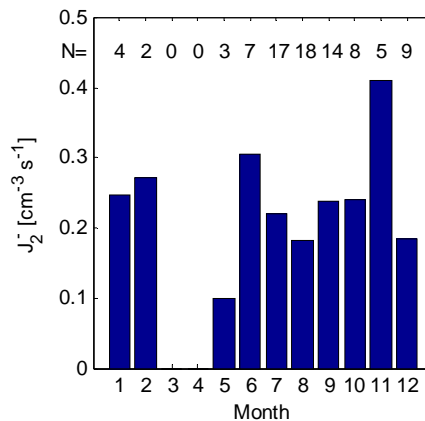
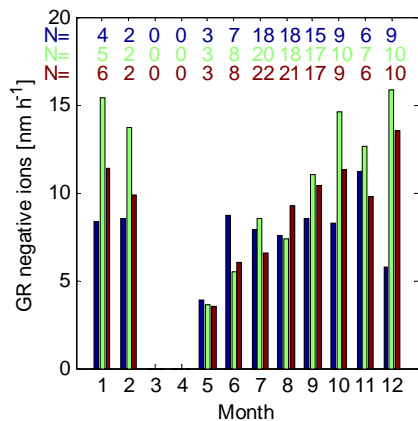
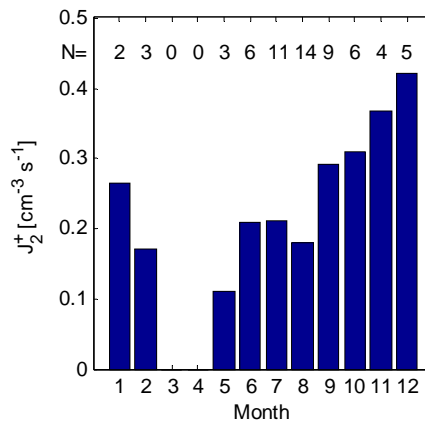
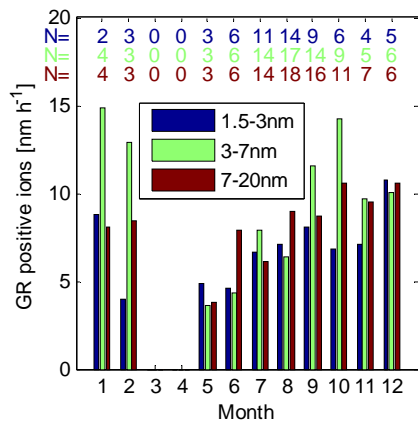
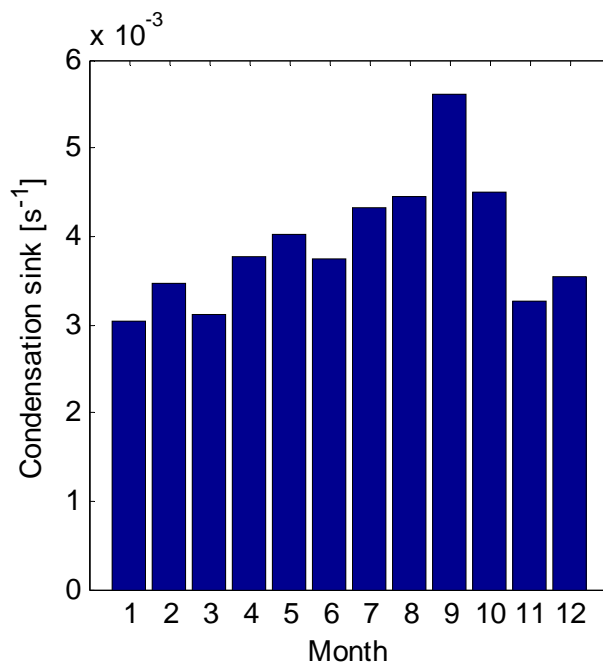


Fig. 5. Positive and negative ion formation and growth rates presented separately for both polarities. The differences between the polarities are negligible.

New particle formation events in semi-clean South African savannah

V. Vakkari et al.

**Fig. 6.** Condensation sink is elevated during the dry season, from May to October.[Title Page](#)[Abstract](#)[Introduction](#)[Conclusions](#)[References](#)[Tables](#)[Figures](#)[◀](#)[▶](#)[◀](#)[▶](#)[Back](#)[Close](#)[Full Screen / Esc](#)[Printer-friendly Version](#)[Interactive Discussion](#)

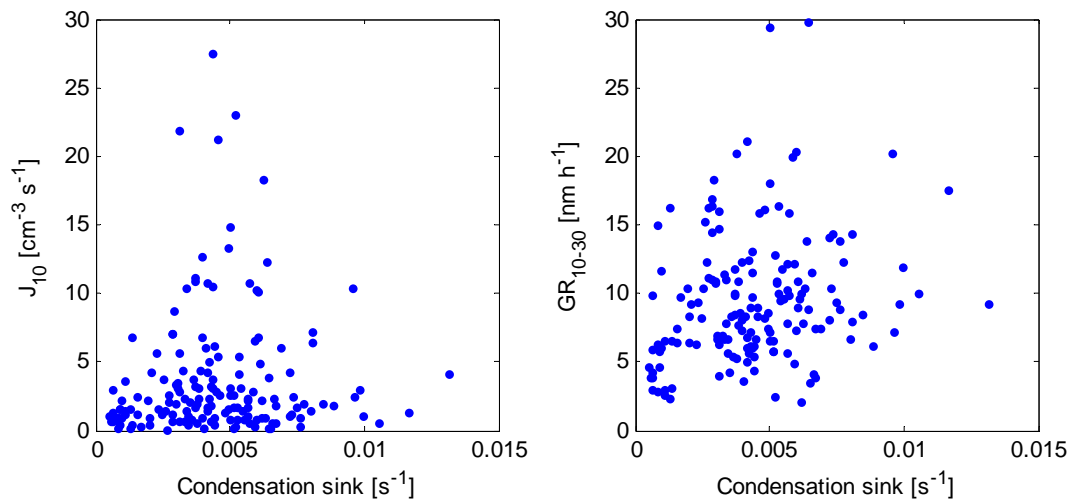


Fig. 7. J_{10} and GR_{10-30} as a function of CS. The GR_{10-30} increase slightly with increasing condensation sink, but the observations are too scattered for a linear fit. The CS is the median during the period when the J_{10} and GR_{10-30} have been determined.

New particle formation events in semi-clean South African savannah

V. Vakkari et al.

Title Page

Abstract Introduction

Conclusions References

Tables Figures

⏪ ⏩

◀ ▶

Back Close

Full Screen / Esc

Printer-friendly Version

Interactive Discussion



New particle formation events in semi-clean South African savannah

V. Vakkari et al.

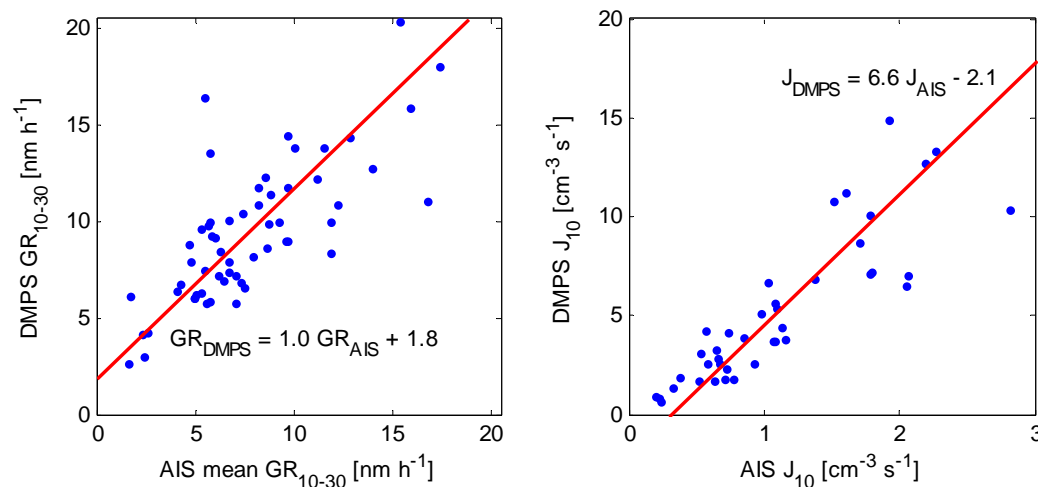


Fig. 8. Comparison of formation and growth rates from DMPS and AIS measurements. The AIS GR_{10-30} is mean of both polarities.

[Title Page](#)
[Abstract](#)
[Introduction](#)
[Conclusions](#)
[References](#)
[Tables](#)
[Figures](#)
[⏪](#)
[⏩](#)
[◀](#)
[▶](#)
[Back](#)
[Close](#)
[Full Screen / Esc](#)
[Printer-friendly Version](#)
[Interactive Discussion](#)

New particle formation events in semi-clean South African savannah

V. Vakkari et al.

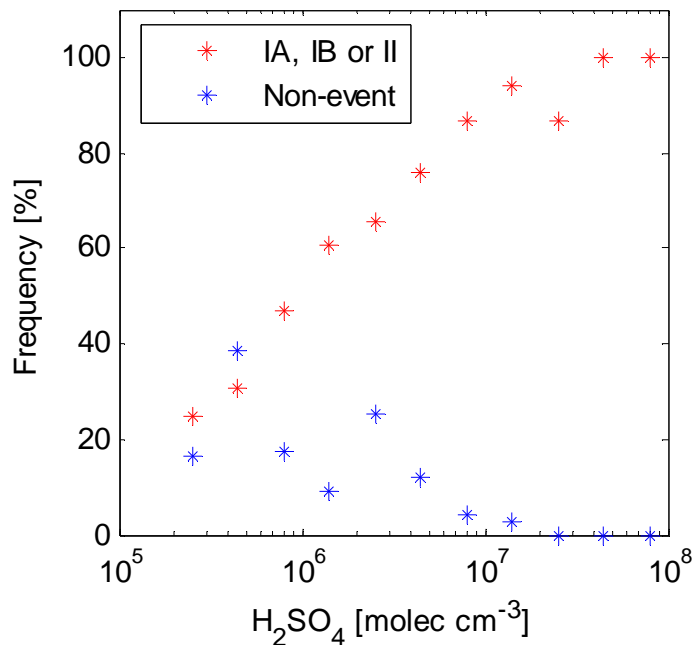


Fig. 9. Frequency of new particle formation and growth days and non-event days as a function of estimated sulphuric acid concentration. The frequency is calculated for logarithmically evenly distributed bins of H_2SO_4 concentration.

[Title Page](#)[Abstract](#)[Introduction](#)[Conclusions](#)[References](#)[Tables](#)[Figures](#)[◀](#)[▶](#)[◀](#)[▶](#)[Back](#)[Close](#)[Full Screen / Esc](#)[Printer-friendly Version](#)[Interactive Discussion](#)

New particle formation events in semi-clean South African savannah

V. Vakkari et al.

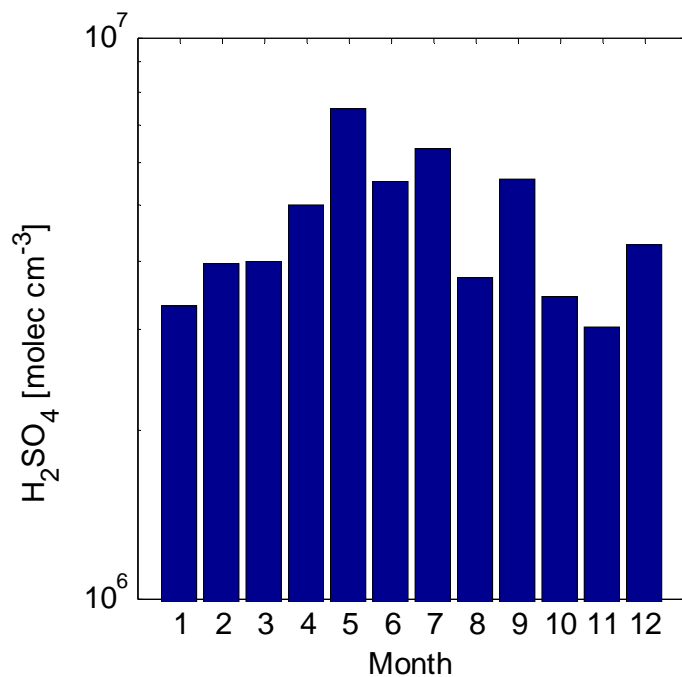


Fig. 10. Seasonal behaviour of the estimated H_2SO_4 concentration. Only values from daytime between 08:00 and 14:00 LT are included.

[Title Page](#)[Abstract](#)[Introduction](#)[Conclusions](#)[References](#)[Tables](#)[Figures](#)[◀](#)[▶](#)[◀](#)[▶](#)[Back](#)[Close](#)[Full Screen / Esc](#)[Printer-friendly Version](#)[Interactive Discussion](#)

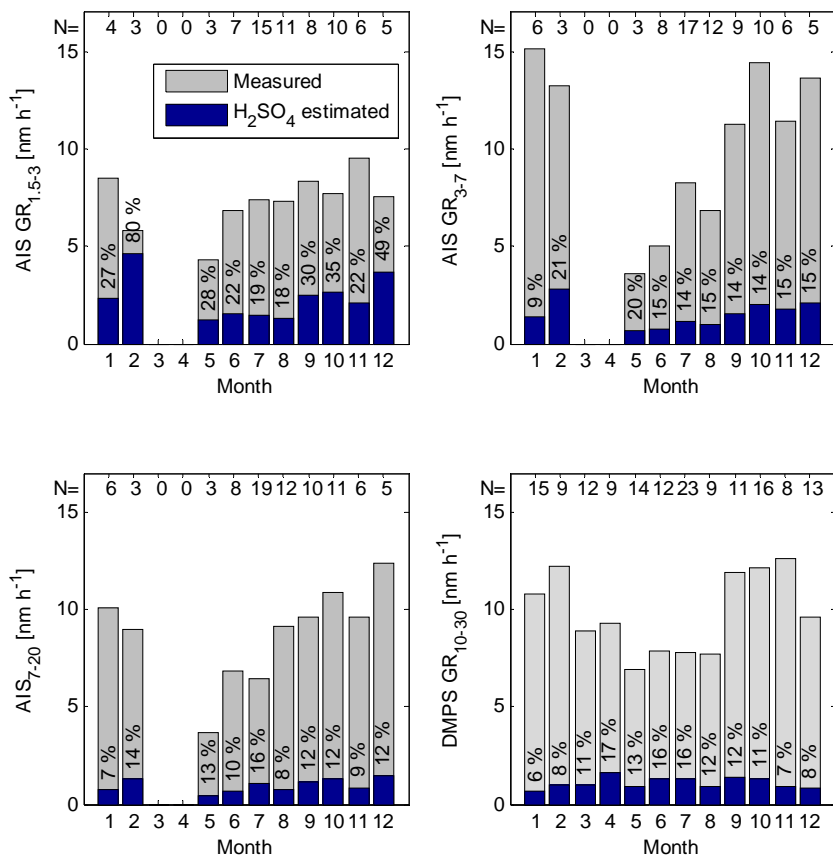


Fig. 11. Observed aerosol particle growth rates and growth rates from the estimated sulphuric acid concentration. The ion growth rates have been averaged over both polarities. The mean of the growth explained by the sulphuric acid as well as the number of events studied is shown for each month and size range.

New particle formation events in semi-clean South African savannah

V. Vakkari et al.

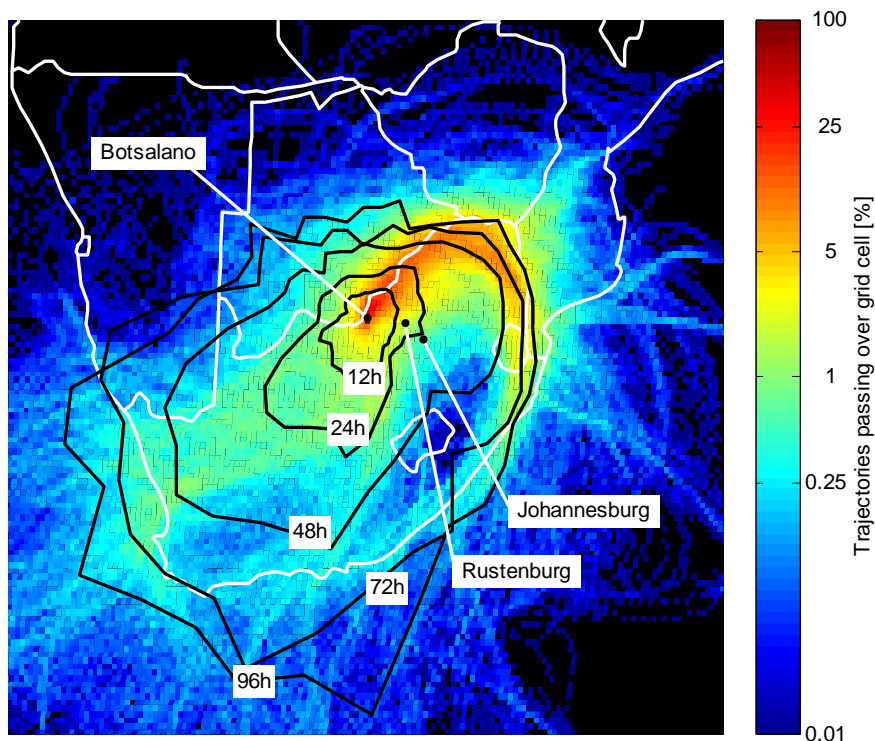


Fig. 12. Back-trajectories in Botsalano. The colour (logarithmic scale) indicates how big a fraction of the back-trajectories passes by each $0.2^\circ \times 0.2^\circ$ cell on the map. The median position of the back-trajectory at 12, 24, 48, 72 and 96 h back in each direction from Botsalano is indicated with the black lines.

Title Page

Abstract

Introduction

Conclusions

References

Tables

Figures

◀

▶

◀

▶

Back

Close

Full Screen / Esc

Printer-friendly Version

Interactive Discussion

New particle formation events in semi-clean South African savannah

V. Vakkari et al.

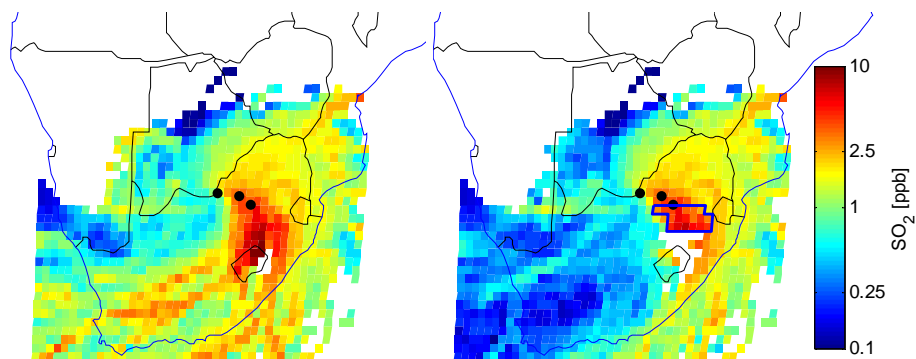


Fig. 13. SO₂ source areas. The black dots represent (from left to right) Botsalano, Rustenburg and Johannesburg. The left-hand map presents the source areas with full-length 96-h back-trajectories. In the right-hand map the trajectories passing over the industrial sources in the Highveld (blue polygon) were cut so that the back-trajectory history before it passed through the polygon was ignored.

[Title Page](#)[Abstract](#)[Introduction](#)[Conclusions](#)[References](#)[Tables](#)[Figures](#)[◀](#)[▶](#)[◀](#)[▶](#)[Back](#)[Close](#)[Full Screen / Esc](#)[Printer-friendly Version](#)[Interactive Discussion](#)

New particle formation events in semi-clean South African savannah

V. Vakkari et al.

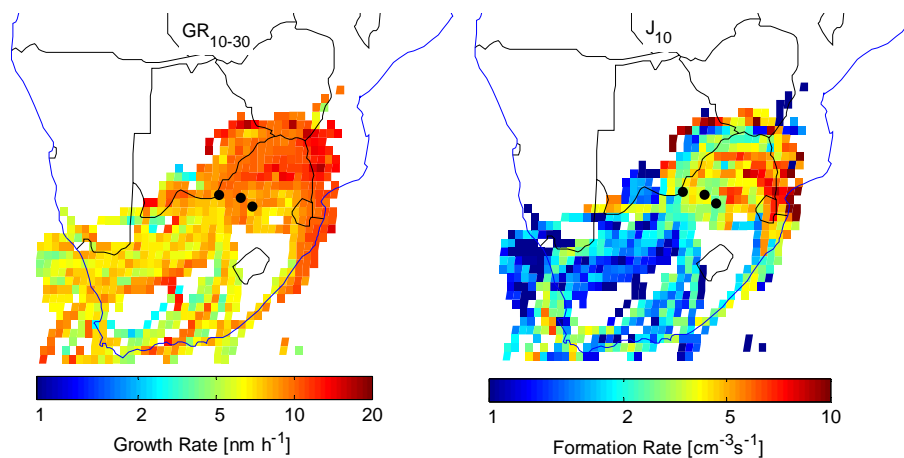


Fig. 14. The source areas of the observed 10 nm formation rate and 10–30 nm growth rate from the DMPS measurements. The black dots represent (from left to right) Botsalano, Rustenburg and Johannesburg. The highest values originate in the north-eastern direction from Botsalano.

[Title Page](#)[Abstract](#)[Introduction](#)[Conclusions](#)[References](#)[Tables](#)[Figures](#)[⏪](#)[⏩](#)[◀](#)[▶](#)[Back](#)[Close](#)[Full Screen / Esc](#)[Printer-friendly Version](#)[Interactive Discussion](#)

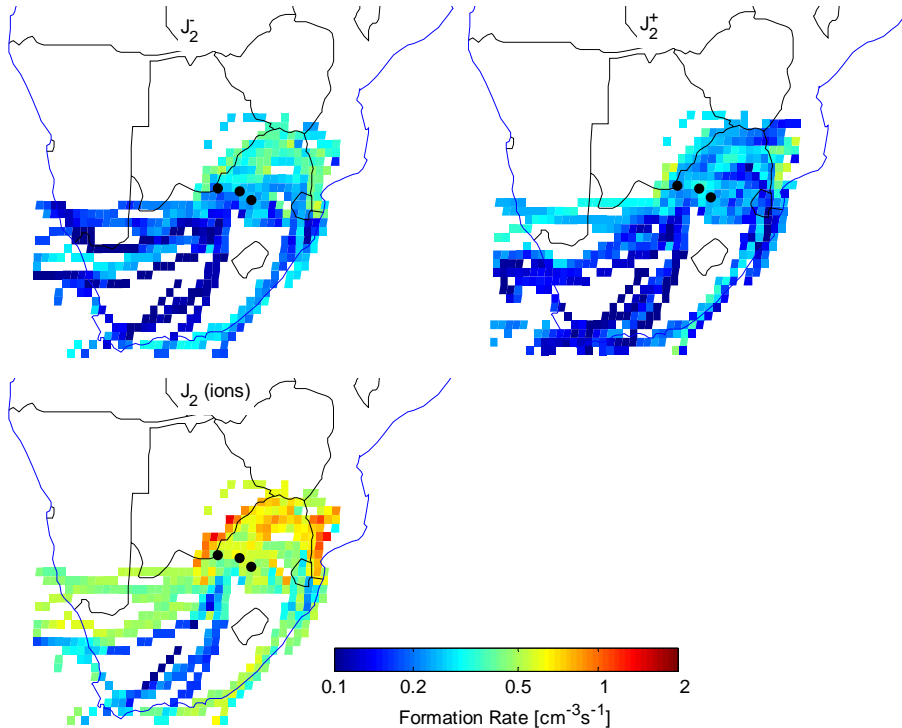


Fig. 15. The source areas of the 2 nm ion formation rates for positive and negative ions separately and the total 2 nm ion formation rate. The black dots represent (from left to right) Botsalano, Rustenburg and Johannesburg. The highest values originate in the north-eastern direction from Botsalano.

New particle formation events in semi-clean South African savannah

V. Vakkari et al.

Title Page

Abstract

Introduction

Conclusions

References

Tables

Figures

◀

▶

◀

▶

Back

Close

Full Screen / Esc

Printer-friendly Version

Interactive Discussion



New particle formation events in semi-clean South African savannah

V. Vakkari et al.

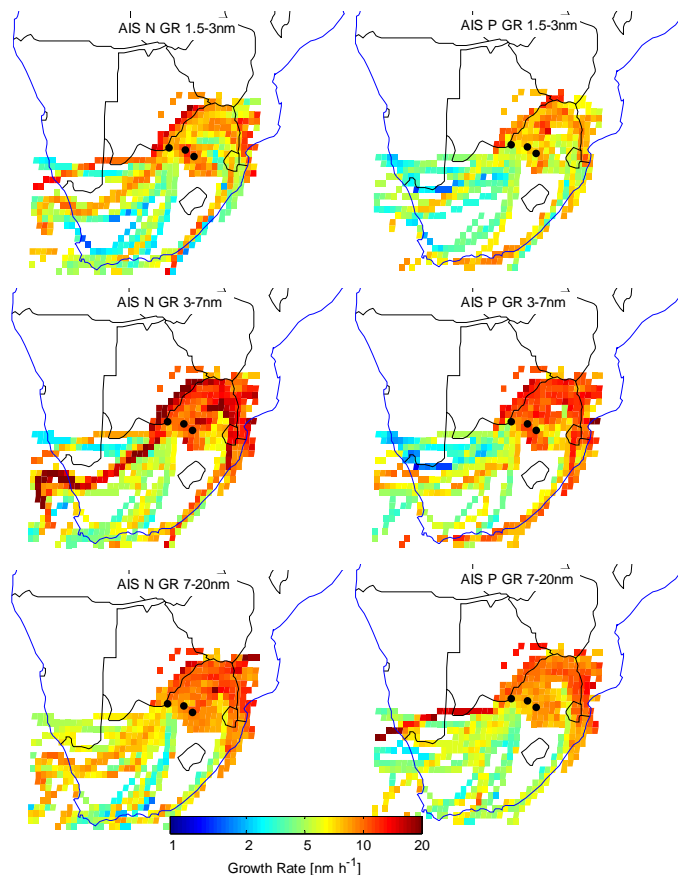


Fig. 16. The source areas of the ion growth rates for size ranges 1.5–3 nm, 3–7 nm and 7–20 nm from the AIS measurements. The black dots on the map represent (from left to right) Botsalano, Rustenburg and Johannesburg. The highest values originate in the north-eastern direction from Botsalano, except for the 1.5–3 nm growth rate, which exhibits higher values also for the Johannesburg-Highveld area.

[Title Page](#)[Abstract](#)[Introduction](#)[Conclusions](#)[References](#)[Tables](#)[Figures](#)[◀](#)[▶](#)[◀](#)[▶](#)[Back](#)[Close](#)[Full Screen / Esc](#)[Printer-friendly Version](#)[Interactive Discussion](#)

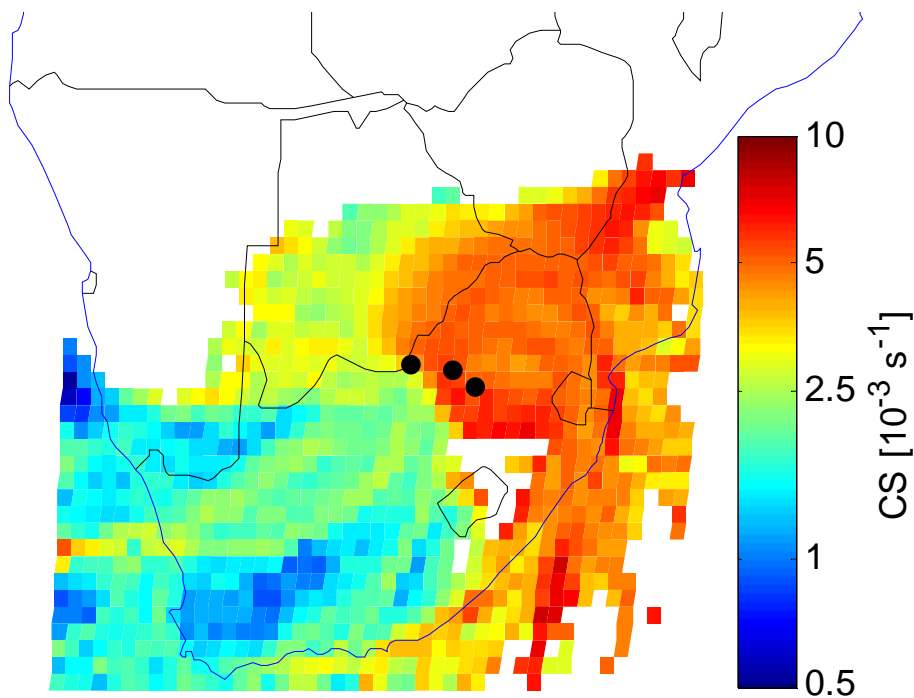


Fig. 17. Condensation sink. The CS originating in the Karoo south west from Botsalano are very low, whereas the CS from north-easterly directions are slightly above the average of $4 \times 10^{-3} \text{ s}^{-1}$. The highest CS originates in the Highveld.

New particle formation events in semi-clean South African savannah

V. Vakkari et al.

Title Page	
Abstract	Introduction
Conclusions	References
Tables	Figures
◀	▶
◀	▶
Back	Close
Full Screen / Esc	
Printer-friendly Version	
Interactive Discussion	



New particle formation events in semi-clean South African savannah

V. Vakkari et al.

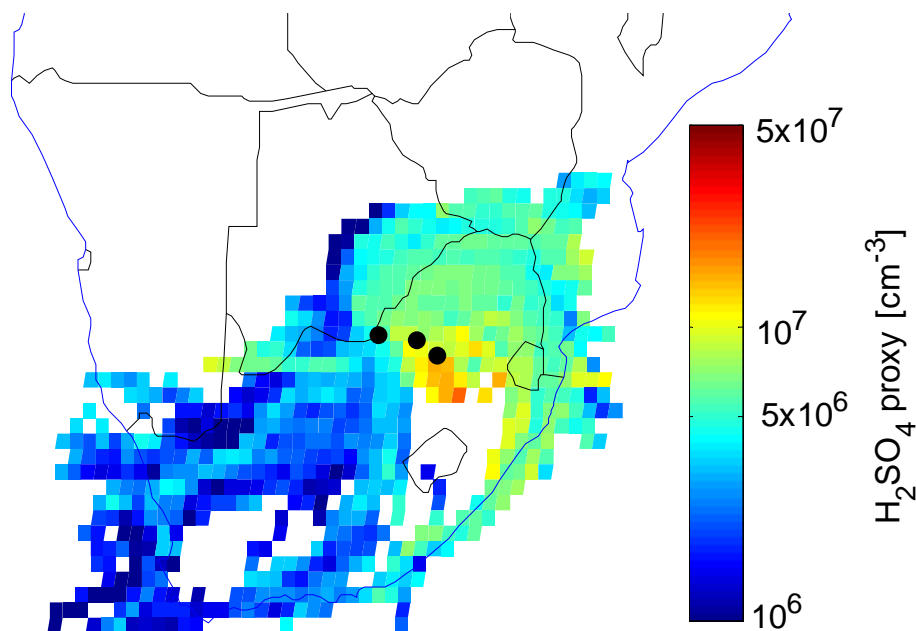


Fig. 18. The source areas of the estimated H_2SO_4 concentration. The black dots represent (from left to right) Botsalano, Rustenburg and Johannesburg.

[Title Page](#)[Abstract](#)[Introduction](#)[Conclusions](#)[References](#)[Tables](#)[Figures](#)[◀](#)[▶](#)[◀](#)[▶](#)[Back](#)[Close](#)[Full Screen / Esc](#)[Printer-friendly Version](#)[Interactive Discussion](#)

New particle formation events in semi-clean South African savannah

V. Vakkari et al.

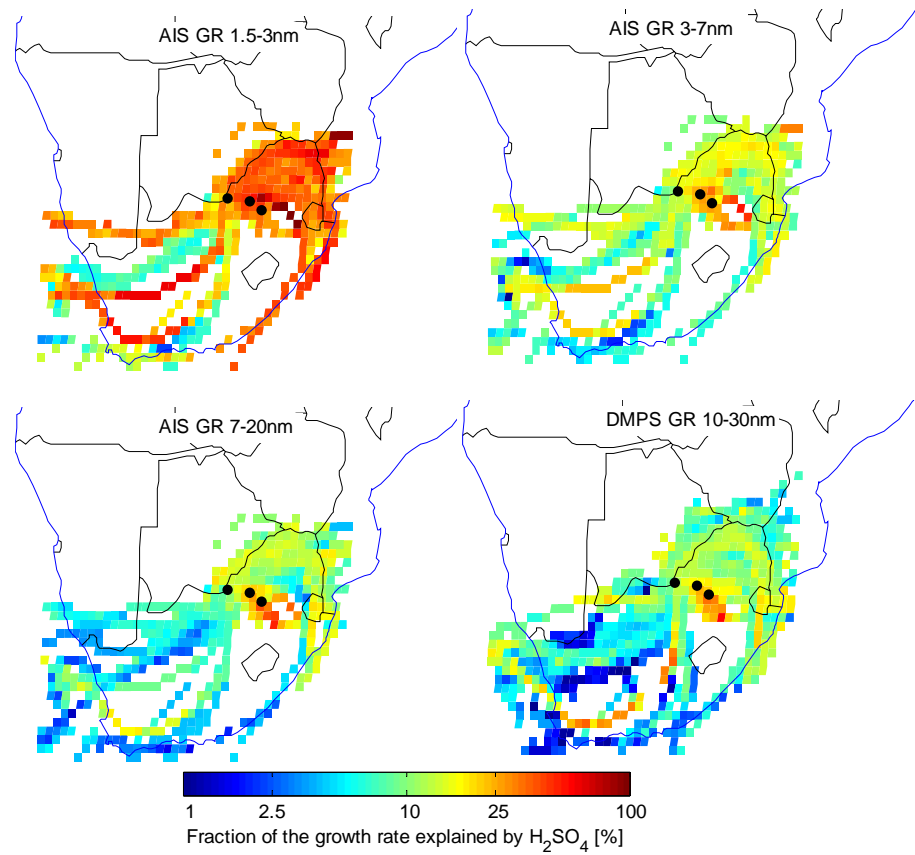


Fig. 19. The source areas of the fraction of growth rate explained by estimated H_2SO_4 . The black dots represent (from left to right) Botsalano, Rustenburg and Johannesburg.

Title Page	
Abstract	Introduction
Conclusions	References
Tables	Figures
◀	▶
◀	▶
Back	Close
Full Screen / Esc	
Printer-friendly Version	
Interactive Discussion	

